Geophys. J. Int. (2005) **160,** 1103–1111 doi: 10.1111/j.1365-246X.2005.02567.x

Tectonic interpretation of aftershock relocations in eastern Papua New Guinea using teleseismic data and the arrival pattern method

P. Tregoning, M. Sambridge, H. McQueen, S. Toulmin* and T. Nicholson*

Research School of Earth Sciences, Australian National University, Canberra ACT 0200, *Australia*

Accepted 2004 December 22. Received 2004 December 17; in original form 2004 September 2

SUMMARY

The arrival pattern (AP) method and teleseismic data have been used to relocate aftershocks following three major ($M_w >= 7.8$) interplate earthquakes that occurred in eastern Papua New Guinea in 2000 November. The first event was an $M_w = 8.0$ strike-slip earthquake that ruptured the Weitin fault over a length of ~100 km. No aftershocks were located in the upper 15 km, suggesting that the accumulated strain was fully released in this event. The two subsequent $M_w = 7.8$ thrust events occurred on the New Britain trench. Wadati–Benioff zones dipping ~20° define the locations of the thrust events at 152°E and 153°E on fault planes with strikes of 75° and 65°, respectively. The plot of aftershocks defines a complex seismic zone beneath New Ireland where events have occurred in the overriding Pacific and South Bismarck plates above the deeper zone of subduction of the Solomon Sea Plate. These events cluster in a broad zone to the northeast of the Weitin fault rather than defining a linear feature that might have been expected following a near-vertical major strike-slip event.

Key words: aftershocks, arrival pattern method, Papua New Guinea, seismology, Weitin fault.

1 INTRODUCTION

Papua New Guinea is one of the most tectonically complex and seismically active regions in the world. Trapped between the convergence of the Pacific and Australian plates, it provides examples of almost every possible type of interplate tectonic boundary. The South Bismarck—Solomon Sea—Pacific Plate triple junction is a complex tectonic area that accommodates left-lateral strike-slip motion between the South Bismarck and Pacific plates (Taylor 1979; Tregoning *et al.* 1998, 1999) and subduction of the Solomon Sea Plate on the New Britain and San Cristobal trenches (Fig. 1a). In addition, the subduction trench undergoes a 70° change in azimuth near the triple junction, and the interaction of faults and trenches in this region is not known. For example, do the faults found in New Ireland join up with the subduction plate boundaries? Has the sharp change in azimuth of the subducting slab produced a tear (or tears) in the subducting slab?

Based on recent GPS results, relative motion between the South Bismarck and Pacific plates is predicted to be ~130 mm yr^{-1} left-lateral slip with ~17 mm yr^{-1} convergence (Tregoning *et al.* 1999). Mapped faults in southern New Ireland include the Weitin fault (Hamilton 1979), which is a strike-slip fault beneath the Weitin and Kamdaru river valleys, and the Sapom fault, which was thought to be part of the transform boundary (Johnson 1979), although Mori (1989) suggested that aftershocks of the 1985 southern New Ireland earthquake showed that it was a thrust fault dipping 40° to 50° to the northeast. Passing beneath the surficial interaction of the South Bismarck and Pacific plates lies the subducted Solomon Sea Plate, clearly imaged in seismic tomography (Hall & Spakman 2002; Tregoning & Gorbatov 2004) and with a well-defined Wadati–Benioff zone of seismicity extending down to 400 km (e.g. Denham 1969; Pascal 1979).

Accurate earthquake locations could potentially reveal some of the tectonic features of the Papua New Guinea region, although the epicentres in available global seismicity catalogues are not accurate enough to provide sufficient resolution. For this reason, we used the arrival pattern (AP) method (Nicholson *et al.* 2002) and multiple phases, not routinely used in solutions of other catalogues, to improve the accuracy of aftershocks following three major earthquakes in 2000 November.

The interpretation of aftershocks to investigate the dynamics of seismic events is a technique that has been used to great advantage. In particular, aftershocks can provide information that leads to the identification of fault rupture planes, thereby permitting the focal mechanisms of events to be determined (e.g. Stein & Lisowski 1983; Hauksson & Jones 1991; Beroza & Zoback 1993). Most studies of aftershocks rely principally upon seismic data recorded on local networks, usually installed immediately after a major seismic event. However, when no local seismic network data have been collected, aftershocks can only be relocated using teleseismic data recorded by global networks. Despite the high frequency of large earthquakes in Papua New Guinea (4 to 20 events of $M_w > 6$ each year since

*Now at: the School of Earth Sciences, Victoria University of Wellington, Wellington, New Zealand.

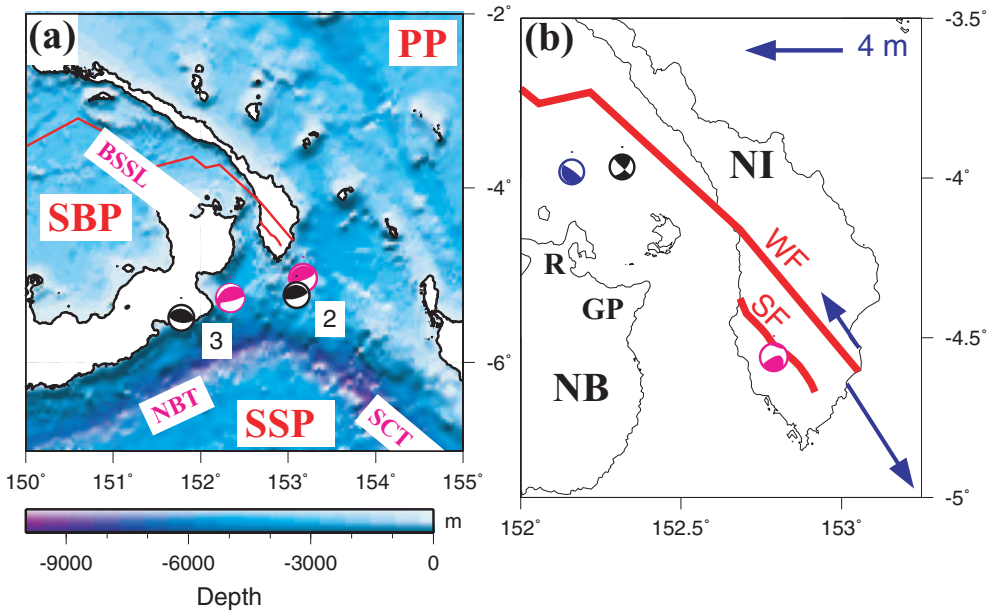

Figure 1. (a) Map of eastern Papua New Guinea showing the bathymetry and tectonic boundaries. Focal mechanisms of National Earthquake Information Center (NEIC; black) and Harvard Central Moment Tensor (CMT; pink) are shown for the $M_w = 7.8$ thrust events that occurred on 2000 November 16 (labelled 2) and 17 (labelled 3). (b) Focal mechanisms for the $M_w = 8.0$ left-lateral event of 2000 November 16. GPS coseismic displacements measured at the two monitoring sites closest to the Weitin fault are plotted as arrows. Note that the observed coseismic displacement includes the possible displacements caused by the two major thrust events as well as the left-lateral rupture of the Weitin fault. The revised NEIC focal mechanism is plotted in blue. Bismarck Sea seismic lineation (BSSL); Gazelle peninsula (GP); New Britain (NB); New Britain trench (NBT); New Ireland (NI); Pacific Plate (PP); Rabaul (R); South Bismarck Plate (SBP); San Cristobal trench (SCT); Sapom fault (SF); Solomon Sea Plate (SSP); Weitin fault (WF).

1976), there are rarely rapid deployments of local seismic networks to record aftershock patterns. In fact, the only known studies that used seismic data from temporary deployments of seismometers were studies of the Rabaul volcanic zone (e.g. Mori & McKee 1987; Finlayson *et al.* 2003; not a post-seismic response), a study of aftershocks following the 1985 New Ireland earthquake (Mori 1989), a microseismic study of the Lae seismic zone (Kulig *et al.* 1993; not a post-seismic response) and a study of aftershocks of the 1998 Sissano earthquake (Hurukawa *et al.* 2003).

2 2000 NOVEMBER EARTHQUAKE SEQUENCE

On 2000 November 16, an $M_w = 8.0$ earthquake occurred in eastern Papua New Guinea near the boundary between the South Bismarck and Pacific plates (Fig. 1). This earthquake (hereinafter called event 1) was followed ~4 h later by an $M_w = 7.8$ thrust earthquake (event 2) on the New Britain trench to the south of New Ireland, the interplate subduction zone between the South Bismarck/Pacific and Solomon Sea plates. 31 h later another $M_w = 7.8$ thrust event occurred (event 3), again on the New Britain trench but ~100 km further west. Aftershocks and subsequent earthquakes continued for several months, with 1400 events of magnitude >3 occurring in the next 6 month. Surficial ruptures (in the form of offset vehicle tracks) were found along the mapped strike of the Weitin fault (Finlayson *et al.* 2003; Itikarai & Tregoning 2003).

Seismic instruments at the Rabaul Volcano Observatory (RVO) saturated on each of the three main events (Itikarai, 2000, private communication); the only other seismometers in Papua New Guinea that recorded the events were located at least 400 km away and are included in the teleseismic observation data set. No local seismic network was subsequently installed in southern New Ireland to record the pattern of aftershocks; therefore, the only seismic data that are available to locate the earthquakes are global teleseismic data and phase arrivals recorded by RVO seismometers that captured the smaller events. While the local data may assist in estimating event locations, the data are not publically available and the events occurred outside the geographical coverage of the local array. Furthermore, the array sits above a low-velocity caldera, which may introduce systematic errors in locations. In this study, we make use of only global teleseismic data to locate the aftershocks.

3 TELESEISMIC DATA AND EVENT LOCATIONS

Algorithms used to relocate aftershocks are commonly written for the cases where data from local seismic networks are available (e.g. HYPODD, Waldhauser & Ellsworth 2000) and are unsuitable for hypocentre locations using teleseismic data recorded at distant stations. An exception is the joint hypocentre determination (JHD) method (Dewey 1971, 1983) in which one event is designated a master event and the locations of other events are calculated relative to this master event. This technique has been used successfully in studies of large earthquakes (e.g. the 2000 Wharton Basin earthquake, Robinson *et al.* 2001; the 1996 Biak earthquake, Henry & Das 2002; the 1998 Antarctic Plate earthquake, Henry *et al.* 2000). The limitation of using a master event is that errors in its location will map directly into the values of all events calculated relative to it.

The tectonic interpretations that can be made using event locations by the Harvard Central Moment Tensor (CMT; e.g. Dziewonski & Woodhouse 1983), International Seismological Centre (ISC; ISC 2001) and National Earthquake Information Center (NEIC) catalogues are limited in Papua New Guinea by the fact that the depths of

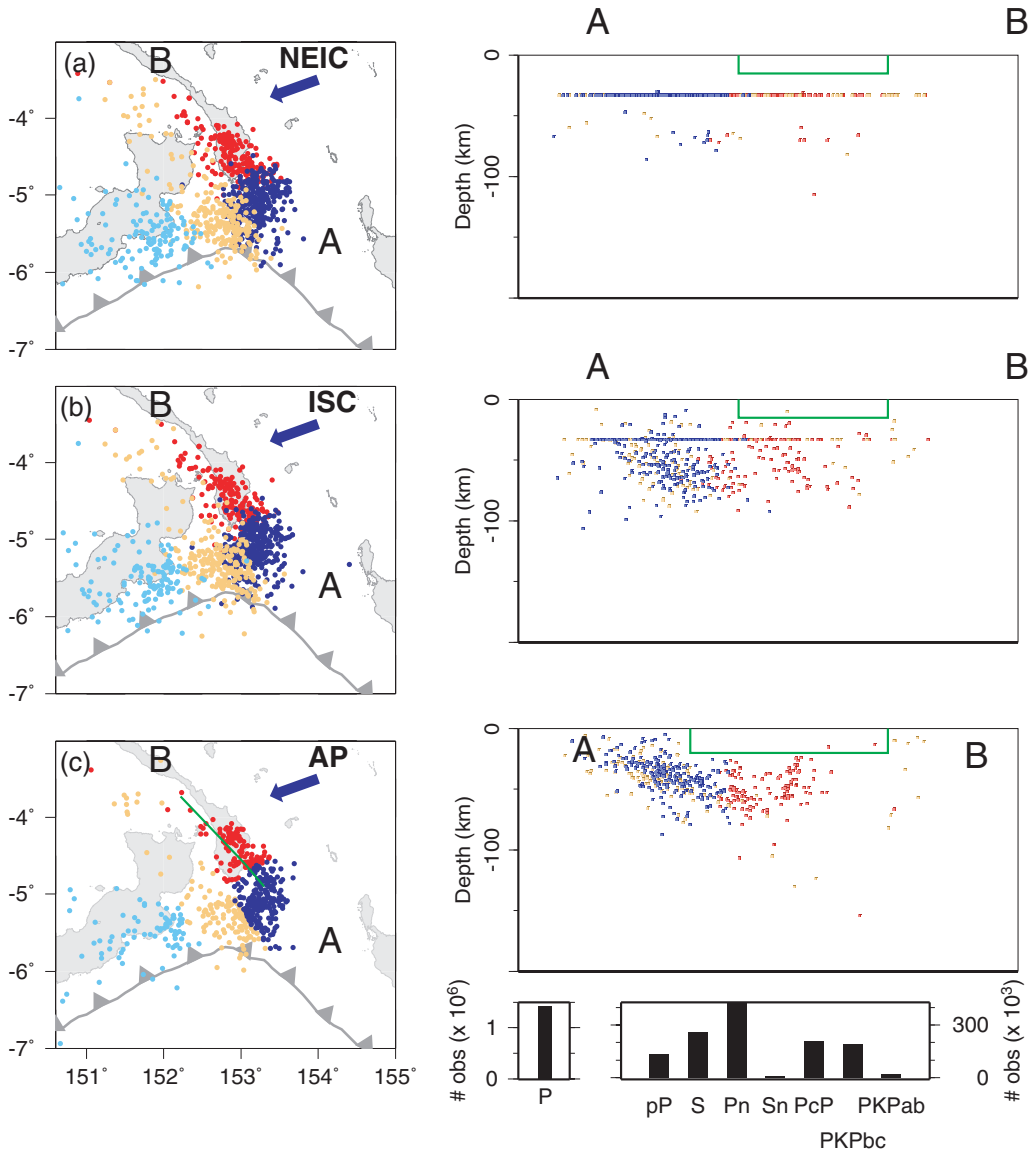

Figure 2. Epicentres of earthquakes from 2000 November 16 to 2001 May 31 from (a) National Earthquake Information Center (NEIC), (b) International Seismological Centre (ISC) catalogues and (c) estimates using the arrival pattern (AP) method (*P* wave plus seven additional phases). Only the events deemed well resolved in the AP method have been plotted as well as only the locations of the corresponding events from the other two sources. Colour-coding of events correspond to differing geographical regions, with arbitrary boundaries of colour-coded zones shown for the AP events: events near the Weitin fault (red), events near the New Britain trench (mustard), events near both features (blue) and events further west associated with the second thrust event (light blue). Cross-sections show events projected onto plane A–B when viewed in the direction of the arrow. The total number of phase observations used in the AP solutions are shown. Events shown contain observations of at least one (but not necessarily all) of the additional phases listed. The location of the Weitin fault is plotted indicatively in green as a rectangle to a depth of 20 km. No vertical exaggeration.

the events are often fixed when trade-offs with origin time cannot be resolved (Aki & Richards 1980). The NEIC locations show horizontally striated patterns (that do not match any likely tectonic regime) with little depth-dependent structure (Fig. 2a). The hypocentres of the ISC catalogue (Fig. 2b) show some depth resolution but there are no clear tectonic features highlighted by the aftershock patterns. There are insufficient earthquakes in the Harvard CMT catalogue (magnitudes >5) to identify any tectonic features.

The NEIC fast moment tensor solution for event 1 (shown in Fig. 1b) shows that the rupture initiated to the northeast of Rabaul. If one extends the fault rupture from the epicentre using the azimuth of the fault plane from the original NEIC focal mechanism (strike = 134°, dip = 87°, rake = 26°) then the rupture passes between the Weitin and Sapom faults. A subsequent NEIC focal mechanism solution (shown in blue in Fig. 1b) is that of a normal fault (strike = 126°, dip = 82°, rake = 79°) and does not match the local tectonic setting.

There is no consensus on the nature of the mapped faults in southern New Ireland. Mori (1989) concluded from an aftershock sequence in 1985 that the Sapom fault was a thrust fault that accommodated convergence between the South Bismarck and Pacific plates. From relocations of event 1, and earthquakes before and after 2000 November 16, Rham & Das (2003) concluded that the Sapom fault had ruptured with pure left-lateral strike-slip on a vertical fault

plane. Clearly, accurate absolute event locations could provide valuable evidence to aid in the identification of the locations of the active faults in the region.

Two types of database information are used in the following sections: arrival times of seismic waves and hyopcentre locations. For clarity, below we refer to assemblages of arrival time observations as observation catalogues and suites of hypocentre coordinates as event catalogues, with the particular catalogue referred to by name. The catalogues used include the Harvard CMT event catalogue (e.g. Dziewonski & Woodhouse 1983), the ISC observation and event catalogues (ISC 2001), the NEIC observation and event catalogues (accessible through the web site at http://neic.usgs.gov/neis/tours/neic˙bulletins.html), and the EHB observation and event catalogues (Engdahl *et al.* 1998): where the EHB observations are the same as the ISC observations but the hypocentres have been estimated in a process that included additional phases.

4 ARRIVAL PATTERN METHOD

With the recently developed AP method (Nicholson *et al.* 2002), one compares phase arrival times of a new event with those of previous events whose positions are assumed to be known (see below) and, by interpolation of a misfit function based on these comparisons, estimate the location of the new event. Effectively, traveltimes predicted by an Earth model are replaced by an ensemble of observation times from previous events (although it is recognized that the locations of the previous events have been estimated using traveltimes predicted by an Earth model; therefore, the AP method is not completely free of an Earth model). The closer a new event lies to a previous event, the smaller will be the differences in the phase arrival times at any particular station for the same phases; hence, the misfit function will be smaller near that event. The solutions are dependent upon the accuracy of the event locations in the database, although the random errors in the estimates of new locations are smaller by a factor of 2 than those associated with the hypocentres contained in the database of previous events. That is, the median new location error is approximately 50 per cent of the median database error (Nicholson *et al.* 2002). Therefore, one can estimate locations of new events with greater accuracy than the accuracies of the events contained in the catalogue. One limitation of the AP method is that it interpolates (and cannot extrapolate) the misfit function at the previous events; therefore, the new event must be contained within the geographical region covered by previous events with matching phases.

It is difficult to assess statistically the uncertainties of the estimated event locations using the AP method because of the complex nature of random and systematic errors affecting seismic observations. Nicholson *et al.* (2002) addressed this issue to some extent by using Monte Carlo procedures (*ibid*) for many events in many different regions, and concluded that the likely 95 per cent confidence ellipse lay approximately at the 2-s contour around the event (approximately 10 km). It is not feasible to perform Monte Carlo simulations for every one of the 1400 aftershocks that occurred; therefore, we assume that the conclusions of Nicholson *et al.* (2002) are valid here as well. Another means of assessing the accuracy of the solutions is by looking at the resolution of tectonic structures evidenced by the aftershock locations. While such an assessment can only be subjective, the results shown below demonstrate clearly that the event locations from the AP analysis reveal more structure than do other location sets. No clustering algorithms have been employed to generate the suite of event locations; rather, each individual aftershock epicentre and depth has been estimated independently.

We used arrival times from the NEIC catalogue and locations of previous events from the EHB catalogue to relocate the events after 2000 November 16. An event that has observations in common with many catalogue events and is surrounded geographically by the catalogue events is more likely to be located accurately than one that lies on the edge of the catalogue events or, even worse, lies outside the catalogue events. Furthermore, one can have greater confidence in a solution if there is a clear decrease in the misfit function at each of the catalogue events as one moves towards the solution location. That is, if there is a clear bull's-eye pattern of the misfit function.

Below, we describe modifications that we implemented in the original algorithm of Nicholson *et al.* (2002).

4.1 Phase selection

Both the Engdahl catalogue of observations and the NEIC observations of aftershocks are heavily dominated by *P*-wave arrival times, with only ∼10 per cent of observations being for other phases. It is well known that the use of the arrival times of some of the additional phases (e.g. *pP*) significantly improve the accuracy of depth estimates; therefore, we chose to relocate only events that contained at least one additional phase observation recorded by at least one station in addition to the *P*-wave arrival times. We used additional phase observations of type *S*, *Pn*, *Sn*, *pP*, *PcP*, *PKPbc* and *PKPab* and weighted the observations as described by (Nicholson *et al.* 2004 table 1).

Fig. 3 shows the locations of aftershocks using various selections of arrival phases, starting with only *P* phases. Very few *pP* arrivals were recorded at the teleseismic stations; therefore, fewer events were located using only *pP*- and *P*-wave arrivals (Fig. 3b). The inclusion of *S*-wave arrivals (Fig. 3c) highlights clearly a zone of seismicity dipping to the north at ∼20°. Also, there appears to be another zone of seismicity further north and above the Wadati–Benioff zone. This is discussed further in Section 6.

The inclusion of yet more phases does not alter significantly the resulting pattern of seismicity (compare Fig. 2c computed with seven additional phases with Fig. 3d where only four additional phases were used). In general, *P*-wave observations form 53 per cent of the total with *Pn* (16 per cent) and *S* (10 per cent) being the most prevalent other phases.

4.2 Detecting *pP* observation outliers

It is critical that the phase arrivals used in the AP solutions are accurate and that there are no misidentification errors. Any such errors propagate directly into the calculated misfit function and will affect the accuracy of the new event location. There are many *pP* phase arrivals in both the EHB and the NEIC observation catalogues that are inconsistent with the EHB hypocentre solutions and other *pP* phase observations. We concluded that some of the *pP* arrival times were in error and devised simple filters to remove outlier observations. It is beyond the scope of this paper to investigate the causes of these errors.

Given the arrival times of both the *P*-wave and the *pP* phase at a particular teleseismic station and the distance from the station to the event, it is possible to calculate the depth of the event by interpolating predicted arrival delays based on some Earth model (we used AK135). We calculate the depth derived from this calculation, $Depth_{pP-P}$, for each station where the *pP* arrival time was recorded, thereby producing multiple, independent estimates of the depth of events. It was quite common for depths for a single event calculated

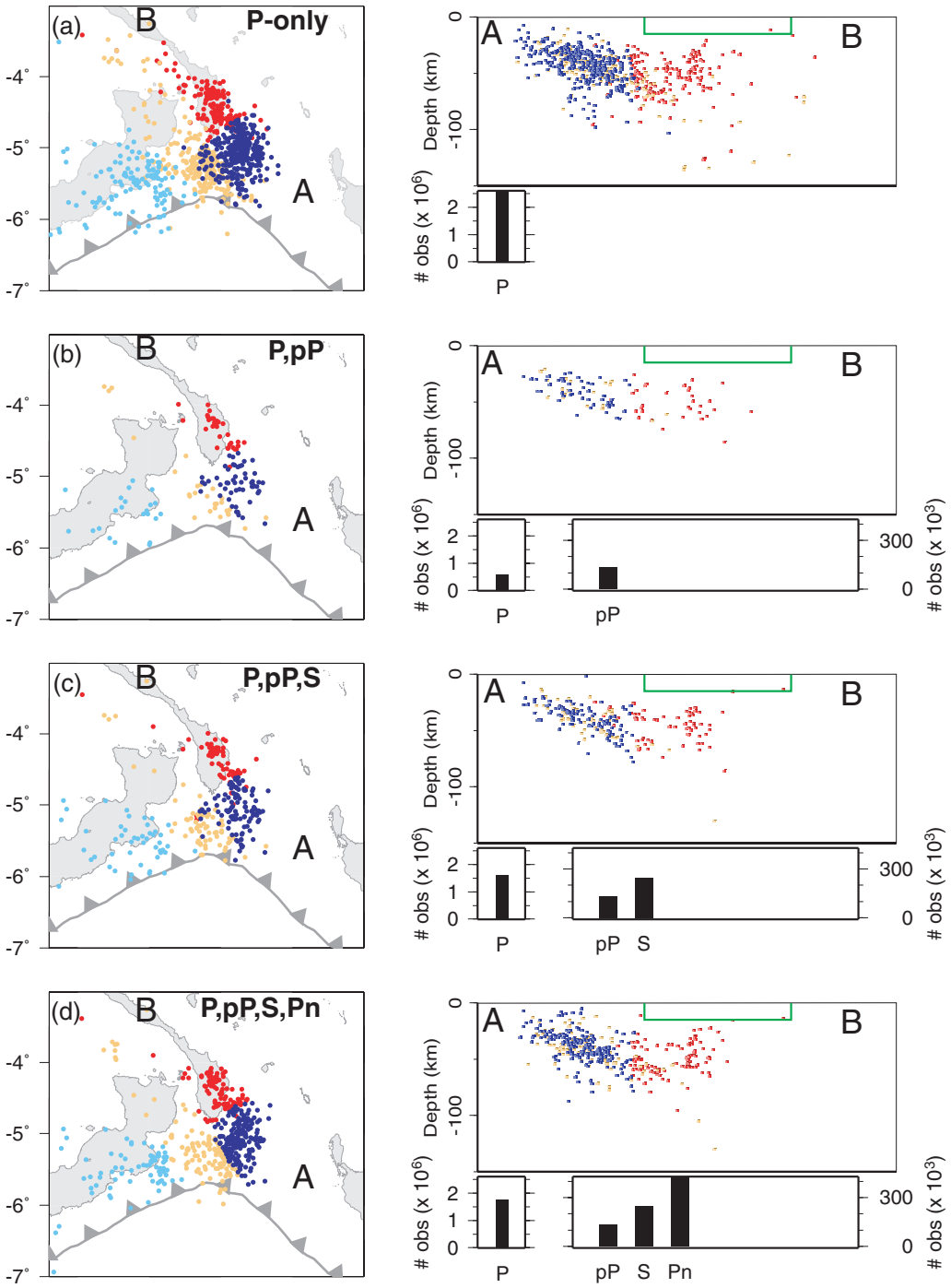

Figure 3. Epicentres and cross-sections using different combinations of additional phases: (a) *P*-wave only; (b) *P* and *pP*; (c) *P*, *pP* and *S*; (d) *P*, *pP*, *S* and *Pn*. Colour-coding is the same as for Fig. 2. No vertical exaggeration.

in this manner to differ significantly from station to station, with the depth differing by up to 50 km from the quoted hypocentre depth in the catalogue (Fig. 4). We found that when the depth estimates of $Depth_{pP-P}$ from all stations had a standard deviation of less than 5 km, the depth estimates from each station were within 10 km of the hypocentre depth, indicating consistency between observations and the final location estimate.

We imposed a set of criteria on the observations to eliminate the erroneous *pP* arrival times in observations of both new and catalogue events. We used only *pP* arrival times when at least two seismic stations recorded this secondary phase and the $Depth_{pP-P}$ estimate for each individual station was within 10 km of the hypocentre depth. The *pP* observations that met these criteria were considered the most reliable observations and were subsequently used in the relocations.

4.3 Selection of catalogue events

The selection of the catalogue events can be made according to several criteria. For example, one could make a selection based

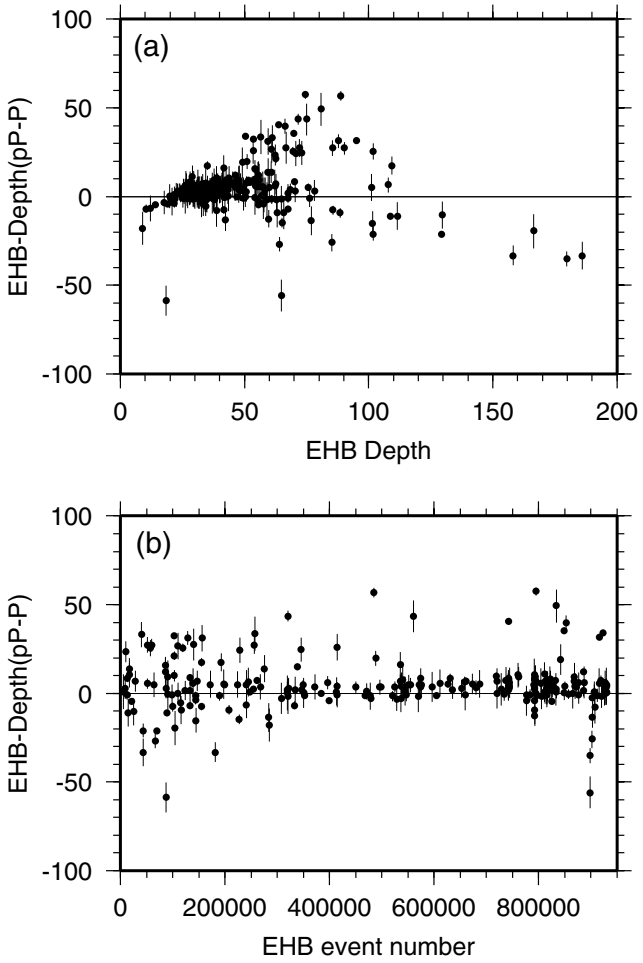

Figure 4. Differences in the EHB catalogue depths of events and those calculated from *pP-P* arrival times (a) as a function of depth and (b) as a function of time. Event 1 occurred in 1964 while the last event in the catalogue occurred on 1999 August 31. 2σ uncertainties are plotted on the difference estimates as calculated from the scatter of the $Depth_{pP-P}$ values.

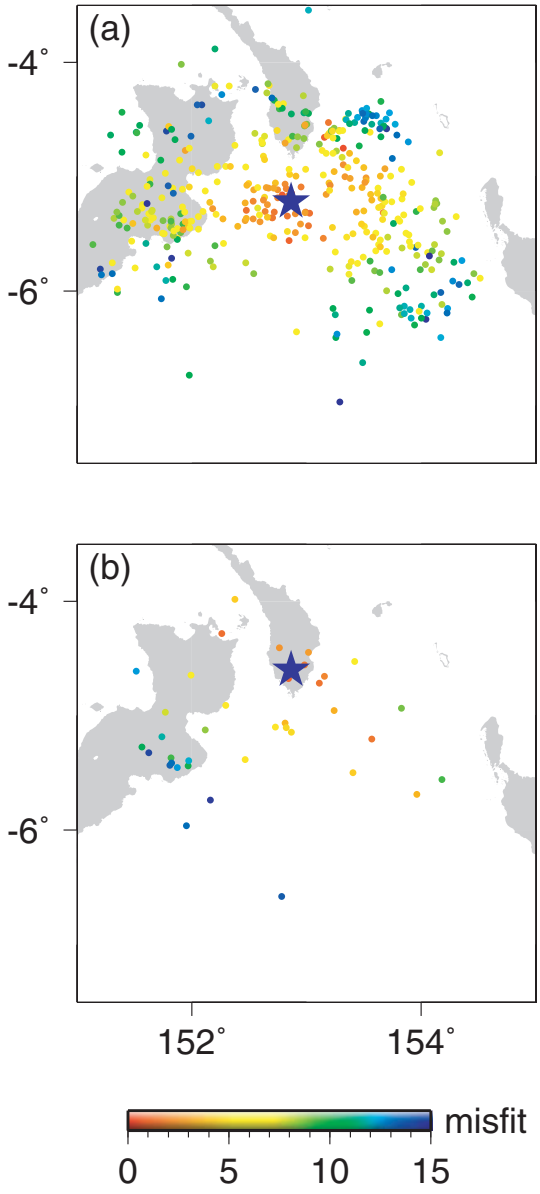

Figure 5. Examples of arrival pattern (AP) estimates of hypocentres: (a) well determined; (b) poorly determined. EHB catalogue earthquakes used in the solution are colour-coded by their misfit values from high (blue) through to low values (red). The AP hypocentre estimate is indicated by a star.

on geographical proximity or on magnitude, starting with either the highest or lowest magnitude events. Our results were generated using up to 400 catalogue events, with the selection based on magnitude starting with the largest events (in fact, selecting the catalogue events with/without a criterion on the magnitude of the events made little difference to the resulting solutions). We relocated only new events with at least 10 matching catalogue events within 400 km of the *a priori* location (the NEIC estimated location).

4.4 Quality of AP solution

Finally, we viewed the solution of each of the relocated events and assessed the pattern of the misfit at the catalogue events. Recall that all events are treated separately with no cluster algorithms employed and no bias towards clustering of events on anticipated tectonic structures. Only new events with a well-defined misfit pattern showing a clear local minimum were considered as being reliable relocated events (e.g. Fig. 5a). Events with sparse observations and no clear bull's-eye pattern were considered unreliable and were rejected (e.g. Fig. 5b). This is a subjective process; however, given that each event was assessed independently and accepted or rejected without any consideration of its actual location, this approach seems reasonable for removing poorly located events without biasing the result. 1006 of the 1400 events passed this assessment criterion and are shown in Fig. 2(c). Only these events and their corresponding solutions from other event catalogues were used when comparing solutions and to interpret the tectonic setting.

The locations estimated with the AP approach and only *P*-wave observations (Fig. 3a) show a tighter clustering of epicentres than either the NEIC (Fig. 2a) or ISC events (Fig. 2b). Fig. 6(a) shows a histogram of changes in locations (epicentre and depth) between the *P*-wave–only locations and the ISC locations (we did not compute the comparison for the NEIC solutions because there are so few events with estimated depths). The locations of around 75 per cent of events were changed by more than 10 km in both depth and epicentre. This may be indicative of the location errors of events in this region in the ISC (and other similar) catalogues derived from

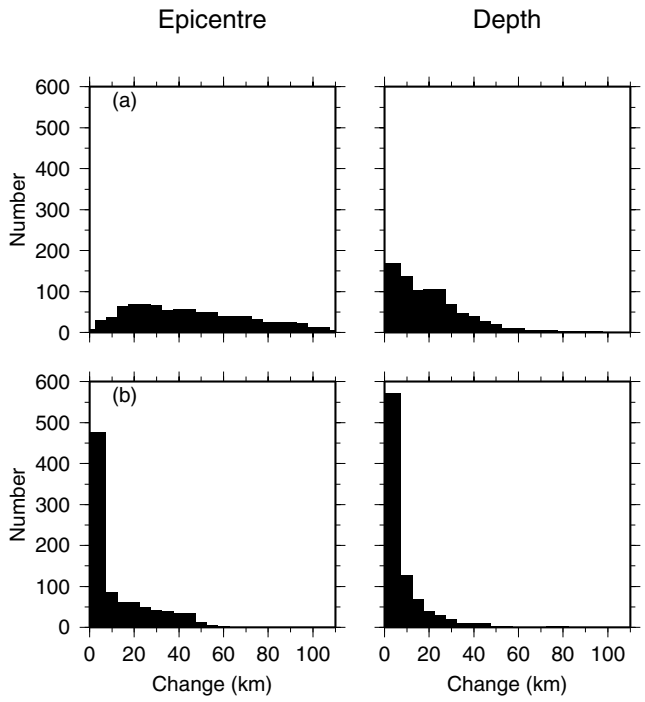

Figure 6. Histograms showing the changes in event locations: (a) between International Seismological Centre (ISC) and arrival pattern (AP; *P*-wave only) solutions; (b) between AP solutions using *P*-wave only and *P*-wave plus seven additional phases.

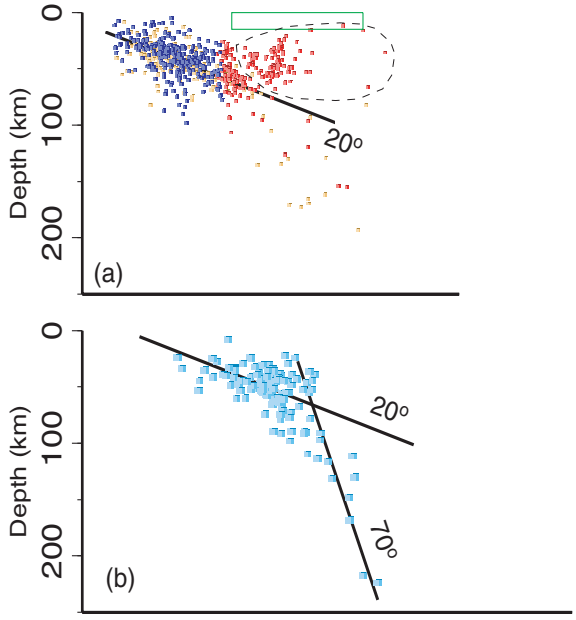

Figure 7. Cross-section of aftershocks most likely associated with the major subduction earthquakes of: (a) event 2 projected onto a vertical plane of azimuth 345°; (b) event 3 projected onto a vertical plane of azimuth 335°. Dip angles of the subducted slab as proposed by Cooper & Taylor (1987) are plotted for comparison and match well the aftershock pattern. Events located inside the dotted region in (a) lie above the subduction zone. Colour-coding of events is the same as in Fig. 2.

only *P*-wave arrival times, although this can only be verified by performing similar comparisons with data sets from either different time periods or nearby areas.

The use of the additional seven phases further refined the AP locations and the histogram of changes is shown in Fig. 6(b). Approximately 40 per cent of epicentres and only ∼20 per cent of depths were changed significantly between AP solutions using only *P*-wave and *P*-wave plus additional phases, with the remainder shifting by less than our expected uncertainty of event location (∼10 km, 2σ). We consider the solutions derived using additional phases to be our best estimates of the epicentres and depths of the aftershocks and it is these locations (Fig. 2c) that we use in the tectonic interpretations below.

The total set of relocated events (including events not shown here within the Solomon Sea Plate and along the San Cristobal trench) can be viewed interactively in three dimensions over the internet (see http://rses.anu.edu.au/geodynamics/gps/NI_eq/png_ap.html).

5 GPS OBSERVATIONS

A regional GPS network had been observed on a sporadic basis since 1998 to monitor deformation across the boundary between the Pacific and South Bismarck plates (Tregoning *et al.* 2000). Re-observations of some of these sites commenced on 2000 November 18. Only four GPS sites, all located near Rabaul on the nearby volcanoes, were recording during the three major earthquakes and for the first 2 d afterwards. The GPS data were analysed using the GAMIT/GLOBK software (Herring 2002; King & Bock 2002) utilizing data from local and global tracking stations. We calculated site displacements of two sites on the southern coast of New Ireland (shown in Fig. 1b) from the difference in coordinates from the last measurement before event 1 (2000 August) and the first occupation after event 3 (2000 December). The re-observations were made after the three major events and after several days of post-seismic relaxation had occurred; hence, the displacements are the sum of three coseismic offsets and possibly three post-seismic relaxation effects. Because of the magnitudes of the displacements (up to 5 m), a careful analysis of the geodetic data is not necessary for estimating the first-order surface deformations caused by the earthquakes and, for simplicity, we ignore any possible second-order post-seismic creep.

Our preliminary results show that event 1 occurred on the Weitin fault (rather than the Sapom fault) with relative left-lateral shear of up to 8 m occurring between two GPS sites separated by <13 km (Fig. 1b). The site northeast of the Weitin fault uplifted ∼18 cm, while the site to the southwest subsided ∼26 cm. An analysis and interpretation of the GPS data set is currently being prepared, including the separation of the effects of the three major earthquakes and numerical values of the coseismic and post-seismic deformations. Here, we present only two critical displacement vectors to demonstrate that event 1 ruptured the Weitin fault and not the Sapom fault.

6 DISCUSSION

The AP algorithm does not force any clustering on the hypocentre estimates yet the events are more clustered than the same events in other catalogues. In this particular tectonic setting, it is reasonable to expect that the events would have occurred on (or very close to) the plate boundary interfaces. We interpret the enhanced clustering of the events as indicating that our estimates of hypocentre locations are more accurate.

A significant number (∼85 per cent) of the aftershocks occurred on the New Britain trench and define a clear Wadati–Benioff zone associated with the subducting Solomon Sea Plate slab. Most of

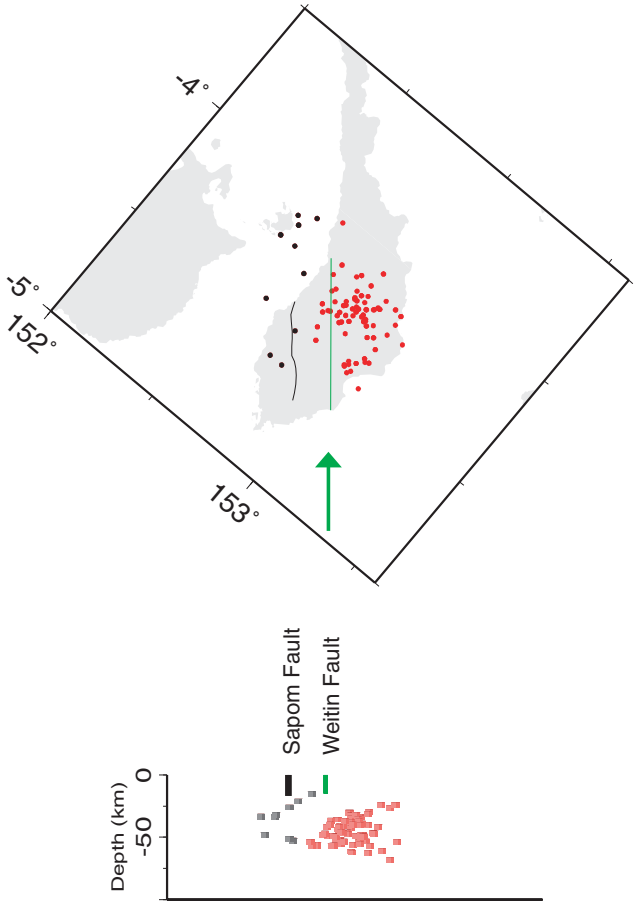

Figure 8. Events near New Ireland that occurred above the subduction zone (i.e. within the dotted region in Fig. 7a), plotted in plan view and in cross-section looking in the direction of the arrow (NW along the strike of the Weitin fault).

the events for which there are CMT focal mechanisms lie in this zone and are thrust-type events, consistent with interplate subduction earthquakes. Coulomb stress failure calculations show that the southward displacement of the overriding South Bismarck Plate caused by event 1 increased the shear stress on the nearby subduction zone, initiating the subsequent thrust events (Park & Mori 2003). Aftershocks occurred to a depth of 230 km.

The dip angle of the subducting Solomon Sea Plate slab has been characterized previously to be ∼20° to a depth of 60 km, beyond which it steepens to 70°–75° (Cooper & Taylor 1987). The aftershocks near 152°E support this earlier conclusion; however, further east it is possible that the dip of the slab becomes shallower as it approaches the 70° change in azimuth of the trench (Fig. 7). (Given the complex nature of the geometry of these tectonic features, it is extremely difficult to portray in 2-D figures. A rotating, 3-D image of the aftershock locations can be viewed at http://rses.anu.edu.au/geodynamics/gps/NI_eq/Nov00.html) The deeper earthquakes near 153°E may have occurred on either the northwest- or northeast-dipping segments of the slab, which may account for the apparent smearing of the events over a broad zone (Fig. 7a) rather than defining a sharp, linear descending slab as seen further west (Fig. 7b).

One result of our relocation of events was that, while some events located on the subducting slab are shallow, no events are found in the top 20 km of the lithosphere along the Weitin fault. Indeed, nearly all the events geographically located in southern New Ireland appear to be related to the subduction process or to have occurred above the subduction interface but at depths greater than 20 km. The majority of the aftershocks in New Ireland that are located above the subduction zone do not lie beneath the Sapom fault but are clustered to the east of the Weitin fault; however, they do not define a linear zone of seismicity as might be expected following a near-vertical strike-slip event (Fig. 8, see also a rotating figure at http://rses.anu.edu.au/geodynamics/gps/NI_eq/weit.html).

The shallow rupture of the Weitin fault may have reactivated many smaller faults and older subduction-related fractures (Mori 1989) in the upper plates. Aftershocks following the $M_w = 8.0$ event do not provide clear information about the locations of the major features and cannot be used to confirm definitively whether the Weitin fault or Sapom fault ruptured. However, GPS coseismic displacements (Fig. 1b) and observed surface offsets (Finlayson *et al.* 2003; Itikarai & Tregoning 2003) do provide conclusive evidence that the strike-slip event occurred on the Weitin fault.

ACKNOWLEDGMENTS

We thank two anonymous reviewers for helpful comments that improved this manuscript and Lomax for the use of his SEISMICITY VIEWER software for viewing earthquake locations in three dimensions (http://alomax.free.fr/seismicity). Figures were plotted with Generic Mapping Tool (GMT) (Wessell *et al.* 1998).

REFERENCES

Aki, K. & Richards, P.G., 1980. *Quantitative Seismology: Theory and Methods,* Freeman and Co., San Francisco.

Beroza, G.C. & Zoback, M.D., 1993. Mechanism diversity of the Loma Prieta aftershocks and the mechanisms of mainshock-aftershock interactions, *Science,* **259,** 210–213.

Cooper, P. & Taylor, B., 1987. Seismotectonics of New Guinea: A model for arc reversal following arc-continent collision, *Tectonics,* **6,** 53–67.

Denham, D., 1969. Distribution of earthquakes in the New Guinea-Solomon Islands region, *J. geophys. Res.,* **74,** 4290–4299.

Dewey, J.W., 1971. Seismic studies with the method of joint hypocenter determination, *PhD thesis,* University of California, Berkeley.

Dewey, J.W., 1983. Relocation of instrumentally recorded pre-1974 earthquakes in the South Carolina region, in, *Studies related to the Charleston, South Carolina, earthquake of 1886–Tectonics and Seismicity,* Professional Paper 1313, pp. Q1–Q9, ed. Gohn, G.S., US Geological Survey, Denver.

Dziewonski, A.M. & Woodhouse, J.H., 1983. Studies of the seismic source using normal-mode theory, in, *Earthquakes: observation, theory, and interpretation: notes from the International School of Physics 'Enrico Fermi' (1982: Varenna, Italy),* pp. 45–137, eds Kanamori, H. & Boschi, E., North-Holland Publishing Company, Amsterdam.

Engdahl, E.R., van der Hilst, R. & Biland, R.P., 1998. Global teleseismic earthquake relocations with improved travel times and procedures for depth determinations, *Bull. seism. Soc. Am.,* **88**(3), 722–743.

Finlayson, D.M., Gudmundsson, O., Itikarai, I., Nishimura, Y. & Shimamura, H., 2003. Rabaul volcano, Papua New Guinea: seismic tomographic imaging of an active caldera, *J. Volc. Geotherm. Res.,* **124**(3–4), 153–171.

Hall, R. & Spakman, W., 2002. Subducted slabs beneath the eastern Indonesia-Tonga region: insights from tomography, *Earth planet. Sci. Lett.,* **201,** 321–326.

Hamilton, W.B., 1979. *Tectonics of the Indonesian Region,* Professional Paper 1078, US Geological Survey, Washington, p. 345.

Hauksson, E. & Jones, L.M., 1991. The 1988 and 1990 Upland earthquakes—left-lateral faulting adjacent to the Central Transverse Ranges, *J. geophys. Res.,* **96,** 8143–8165.

Henry, C. & Das, S., 2002. The M_w 8.2, 17 February 1996 Biak, Indonesia, earthquake: Rupture history, aftershocks and fault plane properties, *J. geophys. Res.,* **107,** doi:10.1029/2001JB000796.

Henry, C., Das, S. & Woodhouse, J.H., 2000. The great March 25 1998, Antarctic Plate earthquake: Moment tensor and rupture history, *Geophys. J. Int.,* **105,** 16 097–16 119.

Herring, T.A., 2002. *GLOBK global Kalman filter VLBI and GPS analysis program,*Version 10.1, Massachusetts Institute of Technology, Cambridge.

Hurukawa, N., Tsuji, Y. & Waluyo, B., 2003. The 1998 Papua New Guinea earthquake and its fault plane estimated from relocated aftershocks, *Pure appl. Geophys.,* **160,** 1829–1841.

ISC, 2001. *International Seismological Centre, On-line Bulletin,* available at http://www.isc.ac.uk/Bull, International Seismological Centre, Thatcham, UK.

Itikarai, I. & Tregoning, P., 2003. The 16 November 2000 southern New Ireland earthquake and its aftershocks, *Geol. Soc. Papua New Guinea,* Report 2003/1, 16pp.

Johnson, R.W., 1979. Geotectonics and volcanism in Papua New Guinea: a review of the late Cainozoic, *Aust. Bur. Min. Res. J. Geol. Geophys.,* **4,** 181–207.

King, R.W. & Bock, Y., 2002. *Documentation for the GAMIT GPS anaylsis software,*Version 10.1, Massachusetts Institute of Technology, Cambridge.

Kulig, C., McCaffrey, R., Abers, G.A. & Letz, H.L., 1993. Shallow seismicity of arc-continent collision near Lae, Papua New Guinea, *Tectonophysics,* **227**(1–4), 81–93.

Nicholson, T., Sambridge M. & Gudmundsson, O., 2002. Hypocenter location by pattern recognition, *J. geophys. Res.,* **107,** 10.1029/2000JB000035.

Nicholson, T., Sambridge, M. & Gudmundsson, O., 2004. Three-dimensional empirical traveltimes: construction and applications, *Geophys. J. Int.,* **156,** 307–328, doi:10.1111/j.1365-246X.2003.02137.x.

Mori, J., 1989. The New Ireland earthquake of July 3, 1985 and associated seismicity near the Pacific-Solomon Sea-Bismarck Sea triple junction, *Phys. Earth planet. Int.,* **55,** 144–153.

Mori, J. & McKee, C., 1987. Outward-dipping ring-fault structure at Rabaul Caldera as shown by earthquake locations, *Science,* **235,** 193–195.

Park, S. & Mori, J., 2003. *Triggering of large earthquakes in the 2000 New Ireland, Papua New Guinea sequence,* poster presented at the IUGG conference, Sapporo, July.

Pascal, G., 1979. Seismotectonics of the Papua New Guinea-Solomon Islands region, *Tectonophys.,* **57,** 7–34.

Rham, D.J. & Das, S., 2003. *Triggering of thrust aftershocks on the New Britain Trench by the November 16, 2000 M_w 7.9 New Ireland strike-slip earthquake,* poster presented at the IUGG conference, Sapporo, July.

Robinson, D.P., Henry, C., Das, S. & Woodhouse, J.H., 2001. Simultaneous rupture along two conjugate planes of the Wharton Basin earthquake, *Science,* **292,** 1145–1148.

Stein, R.S. & Lisowski, M., 1983. The 1979 Homestead Valley earthquake sequence, California—control of aftershocks and postseismic deformation, *J. geophys. Res.,* **88,** 6477–6490.

Taylor, B., 1979. The Bismarck Sea: Evolution of a back-arc basin, *Geology,* **7,** 171–174.

Tregoning, P. & Gorbatov, A., 2004. Evidence for active subduction at the New Guinea Trench, *Geophys. Res. Lett.,* **31,** L13608, doi:10.1029/2004GL020190.

Tregoning, P. *et al.,* 1998. Estimation of current plate motions in Papua New Guinea from Global Positioning System observations, *J. geophys. Res.,* **103,** 12 181–12 203.

Tregoning, P., Jackson, R.J., McQueen, H., Lambeck, K., Stevens, C., Little, R.P., Curley, R. & Rosa, R., 1999. Motion of the South Bismarck Plate, Papua New Guinea, *Geophys. Res. Lett.,* **26,** 3517–3520.

Tregoning, P., McQueen, H., Lambeck, K., Jackson, R., Little, R., Saunders, S. & Rosa, R., 2000. Present-day crustal motion in Papua New Guinea, *Earth, Planets and Space,* **52,** 727–730.

Waldhauser, F. & Ellsworth, W.L., 2000. A double-difference earthquake location algorithm: Method and application to the northern Hayward fault, California, *Bull. seism. Soc. Am.,* **90**(6), 1353–1368.

Wessell, P., Smith, D., Wessel, P. & Smith, W.H. F., 1998. New, improved version of the Generic Mapping Tools released, *EOS, Trans. Am. geophys. Un.,* **79,** 579.